Published for SISSA by Springer

Received: *September 20, 2017*
Revised: *November 9, 2017*
Accepted: *December 18, 2017*
Published: *January 2, 2018*

Lepton number violating phenomenology of $d = 7$ neutrino mass models

R. Cepedello,[a] **M. Hirsch**[a] **and J.C. Helo**[b,c]

[a] *AHEP Group, Instituto de Física Corpuscular — C.S.I.C./Universitat de València, Edificio de Institutos de Paterna, Apartado 22085, E-46071 València, Spain*

[b] *Departamento de Física, Facultad de Ciencias, Universidad de La Serena, Avenida Cisternas 1200, La Serena, Chile*

[c] *Centro-Científico-Tecnológico de Valparaíso, Casilla 110-V, Valparaíso, Chile*

E-mail: ricepe@ific.uv.es, mahirsch@ific.uv.es, jchelo@userena.cl

Abstract: We study the phenomenology of $d = 7$ 1-loop neutrino mass models. All models in this particular class require the existence of several new $SU(2)_L$ multiplets, both scalar and fermionic, and thus predict a rich phenomenology at the LHC. The observed neutrino masses and mixings can easily be fitted in these models. Interestingly, despite the smallness of the observed neutrino masses, some particular lepton number violating (LNV) final states can arise with observable branching ratios. These LNV final states consists of leptons and gauge bosons with high multiplicities, such as $4l + 4W$, $6l + 2W$ etc. We study current constraints on these models from upper bounds on charged lepton flavour violating decays, existing lepton number conserving searches at the LHC and discuss possible future LNV searches.

Keywords: Beyond Standard Model, Neutrino Physics

ArXiv ePrint: 1709.03397

Open Access, © The Authors.
Article funded by SCOAP[3].

https://doi.org/10.1007/JHEP01(2018)009

JHEP01(2018)009

Contents

JHEP01(2018)009

1 Introduction

A Majorana mass term for neutrinos always implies also the existence of lepton number violating (LNV) processes. The best-known example is neutrinoless double beta decay ($0\nu\beta\beta$), for reviews see [1, 2]. A high-scale mechanism, such as the classical seesaw type-I [3–5], however, will leave no other LNV signal than $0\nu\beta\beta$ decay. From this point of view, models in which the scale of LNV is around the electro-weak scale are phenomenologically much more interesting.

Low-scale Majorana neutrino mass models need some suppression mechanism to explain the observed smallness of neutrino masses. (For a recent review on theoretical aspects of neutrino masses see [6].) This suppression could be due to loop factors [7, 8], or neutrino masses could be generated by higher order operators [9, 10], or both. In this paper, we will study the phenomenology of a particular class of models, namely $d = 7$ 1-loop models [11]. Our main motivation is that $d = 7$ 1-loop contributions to neutrino masses can be dominant only, if new particles below approximately 2 TeV exist. This mass range can be covered by the LHC experiments in the near future, if some dedicated search for the LNV signals we discuss in this paper is carried out.

Lepton number violation has been searched for at the LHC so far using the final state of same-sign dileptons plus jets, $l^{\pm}l^{\pm}jj$. Many different LNV extensions of the standard model (SM) can lead to this signal [12, 13]. However, ATLAS and CMS searches usually concentrate on only two theoretical scenarios, left-right symmetry [14] and the standard

model extended with "sterile neutrinos". Note that these two models lead to the same final state signal, but rather different kinematical regions are explored in the corresponding experimental searches. CMS has published first results from searches at run-II [15] and run-I [16], both for $eejj$ and $\mu\mu jj$ final states, concentrating on the left-right symmetric model.[1] There is also a CMS search for sterile Majorana neutrinos, based on $\mathcal{L} = 19.7/fb$ at $\sqrt{s} = 8\,\text{TeV}$ [18]. ATLAS published a search for $lljj$ based on 8 TeV data, for both SM with steriles and for the LR model [19]. However, only like-sign lepton data was analyzed in [19] and no update for $\sqrt{s} = 13\,\text{TeV}$ has been published so far from ATLAS. No signal has been seen in any of these searches so far and thus lower (upper) limits on masses (mixing angles) have been derived.

Other final states that can test LNV have been discussed in the literature. For example, in the seesaw type-II [20] the doubly charged component of the scalar triplet Δ can decay to either $\Delta^{++} \to l^+l^+$ or $\Delta^{++} \to W^+W^+$ final states. If the branching ratios to both of these final states are of similar order, LNV can be established experimentally [21–24]. No such search has been carried out by the LHC experiments so far. Instead, ATLAS [25–27] and CMS [28] have searched for invariant mass peaks in the same-sign dilepton distributions. Assuming that the branching ratios for ee and/or $\mu\mu$ are large, i.e. $\mathcal{O}(1)$, lower limits on the mass of the $\Delta^{\pm\pm}$ up to 850 GeV [27], depending on the flavour, have been derived. Note that, if only one of the two channels are observed, LNV can not be established at the LHC but the type of scalar multiplet could be still determined [29].

Dimension-7 ($d = 7$) neutrino mass models can lead to new LNV final states at the LHC. The proto-type tree-level model of this kind has been discussed first in [10], in the following called the BNT model. As pointed out in [10] the model predicts the final state $W^\pm W^\pm W^\pm + W^\mp l^\mp l^\mp$. The LHC phenomenology of the BNT model has been studied recently in detail in [30]. Again, as in the case of $W^\pm W^\pm + l^\mp l^\mp$ predicted by the seesaw type-II, no experimental search for this particular LNV final state has been published so far.

At tree-level the BNT model is unique in the sense that it is the only $d = 7$ model that avoids the lowest order $d = 5$ contribution to the neutrino mass, without relying on additional (discrete) symmetries [9, 11]. Recently, we have studied systematically $d = 7$ 1-loop neutrino mass models [11]. These models, while necessarily more rich in their particle content than simple $d = 5$ (or $d = 7$) tree-level neutrino mass models, offer a variety of interesting LNV signals at the LHC, so far not discussed in the literature. As we show below, depending on the unknown mass spectrum, several different multi-lepton final states with gauge bosons up to $W^\pm W^\pm l^\mp l^\mp + l^\pm l^\pm l^\mp l^\mp$ can occur. Note that for such high multiplicity final states one can expect very low SM backgrounds.

Apart from LNV signals, the parameter space of $d = 7$ neutrino mass models can be constrained by a variety of searches. First, neutrino masses and angles should be correctly fitted. Since we now know that all three active neutrino mixing angles are non-zero, this fit leads to certain predictions for lepton flavour violating decays. We therefore discuss also current and future constraints coming from $\mu \to e\gamma$, $\mu \to 3e$ and $\mu \to e$-conversion in nuclei.

[1] CMS has searched also for $\tau\tau jj$ [17]. However, that search is not a test for LNV, since one τ is assumed to decay hadronically.

JHEP01(2018)009

Constraints on our models come also from lepton number conserving LHC searches. The same-sign dilepton searches [25–28], discussed above, can be recasted into lower mass limits valid for our models. In addtion, also multi-lepton searches [31], motivated by the seesaw type-III, can be used to obtain interesting limits. We note in passing that we have also checked that the LNV searches for $lljj$ [15, 19] are currently not competitive for the models we consider in this paper.

The rest of this paper is therefore organized as follows. In the next section, we discuss the basic setup of $d = 7$ models and then present the Lagrangians of our two example models. Section 3 then calculates neutrino masses and constraints from low energy probes. Section 4 discusses LHC phenomenology. We first derive constraints from existing searches, before discussing possible searches for LNV final state. We then close with a short summary and discussion.

2 Theoretical setup: $d = 7$ models

2.1 $d = 7$ neutrino mass models

Before we discuss our example models, it may be useful to recapitulate some basics about Majorana neutrino masses in general and $d = 7$ models in particular. Majorana neutrino masses can be generated from $d = 5 + 2n$ operators:

$$\mathcal{O}^{d=5+2n} = LLHH \times (HH^\dagger)^n \tag{2.1}$$

The lowest order, $d = 5$, is the well-known Weinberg operator [32]. At tree-level, the Weinberg operator has three types of ultra-violet completions [33], known in the literature as seesaw type-I, type-II and type-III. These (simplest) neutrino mass models make use of either a right-handed neutrino (type-I), a scalar triplet (type-II) or a fermionic triplet with zero hypercharge (type-III).

Higher order contributions to neutrino masses are expected to be subdominant, unless the underlying model does not generate $\mathcal{O}^W$.[2] This can be achieved essentially in two ways: either via introducing a discrete symmetry [9] or simply because the particle content of the model does not allow to complete the lowest order operator [10, 11]. We will not be interested in models with additional discrete symmetries here, since such models, although interesting theoretically, usually are based on additional SM singlet states, which leave very little LHC phenomenology to explore.[3] Consider, instead, the BNT model [10]. This $d = 7$ tree-level model introduces a vector-like fermion pair, Ψ and $\bar{\Psi}$ with quantum numbers $\mathbf{3}_1^F$ and a scalar quadruplet $S \equiv \mathbf{4}_{3/2}^S$. (Here and elsewhere we will use a notation which gives the $\mathrm{SU}(2)_L$ representation and hypercharge in the form $\mathbf{R}_Y$ with a superscript S or F, where necessary.) By construction, at tree-level the lowest order contribution to the neutrino masses is $d = 7$, see figure 1. Being higher order, already at tree-level, two new particles are needed in order to generate a neutrino mass. This model has a rich LHC phenomenology [10, 30] and, in particular, generates the LNV final state $W^\pm W^\pm W^\pm + W^\mp l^\mp l^\mp$.

[2] $\mathcal{O}^W$ and higher order operators could give similar contibutions to neutrino masses, if the coefficient of $\mathcal{O}^W$ is small. We are not interested in this case.

[3] "Sterile" neutrino searches at the LHC, see introduction, provide of course constraints on these models.

JHEP01(2018)009

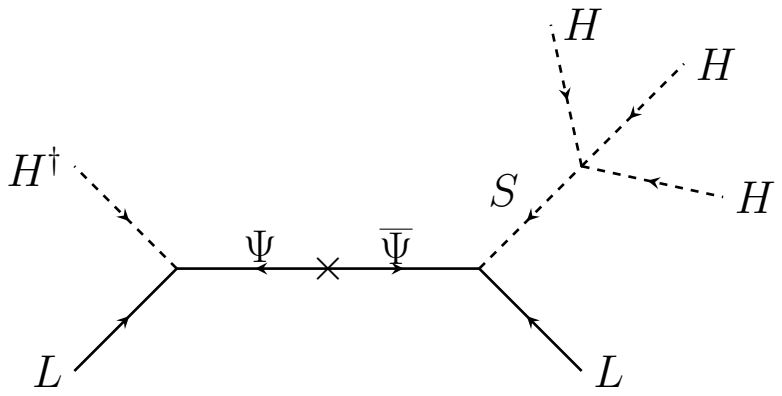

Figure 1. $d = 7$ neutrino mass diagram, for the BNT model [10].

As mentioned in the introduction, the BNT model is unique at tree-level in the sense that no additional symmetries are required to make it the leading contribution to neutrino masses (we call such models "genuine"). In a recent paper [11], we have analyzed systematically $d = 7$ 1-loop models. While there exists a large number of topologies, only a few of them can lead to genuine $d = 7$ models. These topologies can still generate 23 different diagrams, but all models underlying these diagrams share the following common features: (i) five new multiplets must be added to the SM particle content; and (ii) all models contain highly charged particles. In all cases there is at least one triply charged state. Thus, see also the discussion, one expects that all $d = 7$ 1-loop models have rather similar accelerator phenomenology. For this reason, in this paper we concentrate on only two of the simplest example models.[4]

According to [11] one can classify the $d = 7$ models w.r.t. increasing size of the largest $\mathrm{SU}(2)_L$ multiplet. There is one model, in which no representation larger than triplets is needed. All other models require at least one quadruplet. Our two example models, introduced below, are therefore just the simplest realizations of $\mathcal{O}^{d=7}$ at 1-loop, but are expected to cover most of the interesting phenomenology.

Finally, let us mention that the $d = 7$ operator, see eq. (2.1), generates automatically also a 1-loop $d = 5$ neutrino mass:

$$\frac{1}{\Lambda^3} LLHHHH^\dagger \to \frac{1}{16\pi^2}\frac{1}{\Lambda} LLHH \tag{2.2}$$

It is easy to estimate that this loop contribution will become more important than the tree-level if $\Lambda \gtrsim 2\,\mathrm{TeV}$. Our main motivation for the present study is that the LHC can explore large parts of this parameter space.

2.2 Triplet model

Our first example model is the "minimal" 1-loop $d = 7$ model. This model is minimal in the sense that it uses no multiplet larger than triplets. The model adds two new (vector-like)

[4]Strictly speaking this is true only for variants of the $d = 7$ 1-loop models for which the particles appearing in the loop are colour singlets. For a brief discussion for the case of coloured particles see section 5.

JHEP01(2018)009

fermions and three scalars to the standard model particle content:

$$\Psi = \begin{pmatrix} \Psi^{++} \\ \Psi^{+} \\ \Psi^{0} \end{pmatrix} \sim \mathbf{3}_1^F \qquad \eta_1 = \begin{pmatrix} \eta_1^{++} \\ \eta_1^{+} \end{pmatrix} \sim \mathbf{2}_{3/2}^S \qquad \eta_2 = \begin{pmatrix} \eta_2^{+++} \\ \eta_2^{++} \end{pmatrix} \sim \mathbf{2}_{5/2}^S$$
$$\eta_3 = \begin{pmatrix} \eta_3^{++++} \\ \eta_3^{+++} \\ \eta_3^{++} \end{pmatrix} \sim \mathbf{3}_3^S \qquad \psi_1 = \begin{pmatrix} \psi_1^{+++} \\ \psi_1^{++} \end{pmatrix} \sim \mathbf{2}_{5/2}^F.$$

Note that both, Ψ and $\bar{\Psi}$ are needed. The Lagrangian of the model contains the following terms:

$$\begin{aligned} \mathscr{L} = & \left[Y_1 H^\dagger \Psi P_L L + Y_2 \overline{\psi}_1 P_L L \eta_3 + Y_3 \eta_1^\dagger \overline{\Psi} \psi_1 + Y_4 \eta_1 \overline{\Psi} P_L L + Y_5\, e_R \eta_1^\dagger \psi_1 + \text{H.c.} \right] \\ & - M_\Psi \overline{\Psi} \Psi - M_{\psi_1} \overline{\psi}_1 \psi_1 - V_{\text{scalar}}, \end{aligned} \tag{2.3}$$

with the scalar part given by:

$$\begin{aligned} V_{\text{scalar}} = & \, m_H^2 H^\dagger H + m_{\eta_1}^2 \eta_1^\dagger \eta_1 + m_{\eta_2}^2 \eta_2^\dagger \eta_2 + m_{\eta_3}^2 \eta_3^\dagger \eta_3 \\ & + \left[\mu_1\, H \eta_2 \eta_3^\dagger + \mu_2 \eta_1 \eta_1 \eta_3^\dagger + \lambda_2 \eta_2^\dagger H \eta_1 H + \lambda_3\, \eta_1^\dagger \eta_2 \eta_1^\dagger H + \text{H.c.} \right] \\ & + \frac{1}{2}\lambda_1 (H^\dagger H)^2 + \frac{1}{2}\lambda_4 (\eta_1^\dagger \eta_1)^2 + \frac{1}{2}\lambda_5 (\eta_2^\dagger \eta_2)^2 + \frac{1}{2}\lambda_6 (\eta_3^\dagger \eta_3)^2 + \frac{1}{2}\lambda_7 (\eta_3^\dagger \eta_3^\dagger)(\eta_3 \eta_3) \\ & + \lambda_8 (H^\dagger H)(\eta_1^\dagger \eta_1) + \lambda_9 (H^\dagger H)(\eta_2^\dagger \eta_2) + \lambda_{10} (H^\dagger H)(\eta_3^\dagger \eta_3) + \lambda_{11} (\eta_1^\dagger \eta_1)(\eta_2^\dagger \eta_2) \\ & + \lambda_{12} (\eta_1^\dagger \eta_1)(\eta_3^\dagger \eta_3) + \lambda_{13} (\eta_2^\dagger \eta_2)(\eta_3^\dagger \eta_3) + \lambda_{14} (H^\dagger \eta_1)(\eta_1^\dagger H) + \lambda_{15} (H^\dagger \eta_2)(\eta_2^\dagger H) \\ & + \lambda_{16} (H^\dagger \eta_3)(\eta_3^\dagger H) + \lambda_{17} (\eta_1^\dagger \eta_2)(\eta_2^\dagger \eta_1) + \lambda_{18} (\eta_1^\dagger \eta_3)(\eta_3^\dagger \eta_1) + \lambda_{19} (\eta_2^\dagger \eta_3)(\eta_3^\dagger \eta_2) \end{aligned} \tag{2.4}$$

The model contains many charged scalars, but the only neutral scalar is the standard model Higgs.

From the Yukawa couplings only Y_1, Y_2, Y_3 enter the neutrino mass calculation directly, see next section. Similarly, from the scalar terms only the coupling λ_2 and mass term μ_1 and the mass matrix of the doubly charged scalars play an important role. We therefore give here only the mass matrix for the S_i^{++} states. In the basis (η_1, η_2, η_3) it is given as

$$\mathcal{M}^2_{\eta^{++}} = \begin{pmatrix} m^2_{S_1} & -\frac{\lambda_2 v^2}{2} & 0 \\ -\frac{\lambda_2 v^2}{2} & m^2_{S_2} & -\frac{\mu_1 v}{\sqrt{2}} \\ 0 & -\frac{\mu_1 v}{\sqrt{2}} & m^2_{S_3} \end{pmatrix}. \tag{2.5}$$

Here, v is the SM Higgs vacuum expectation value (vev) and:

$$\begin{aligned} m^2_{S_1} &= m^2_{\eta_1} + \frac{\lambda_7}{2} v^2, \\ m^2_{S_2} &= m^2_{\eta_2} + \frac{\lambda_8 + \lambda_{14}}{2} v^2, \\ m^2_{S_3} &= m^2_{\eta_3} + \frac{\lambda_9 + \lambda_{15}}{2} v^2. \end{aligned} \tag{2.6}$$

JHEP01(2018)009

Eq. (2.5) can be diagonalized by

$$\hat{\mathcal{M}}^2_{\eta^{++}} = R^T_{\eta^{++}} \mathcal{M}^2_{\eta^{++}} R_{\eta^{++}}. \tag{2.7}$$

All other mass matrices of the model can be easily derived and we do not give them here for brevity.

2.3 Quadruplet model

Our second example model makes use of the quadruplet S. The full new particle content of the model is:

$$S = \begin{pmatrix} S^{+++} \\ S^{++} \\ S^{+} \\ S^{0} \end{pmatrix} \sim \mathbf{4}^S_{3/2} \qquad \chi_1 = \begin{pmatrix} \chi_1^{++} \\ \chi_1^{+} \end{pmatrix} \sim \mathbf{2}^F_{3/2} \qquad \chi_2 = \begin{pmatrix} \chi_2^{++++} \\ \chi_2^{+++} \\ \chi_2^{++} \end{pmatrix} \sim \mathbf{3}^F_{3}$$

$$\phi_1 = \phi_1^{++} \sim \mathbf{1}^S_2 \qquad \phi_2 = \begin{pmatrix} \phi_2^{+++} \\ \phi_2^{++} \end{pmatrix} \sim \mathbf{2}^S_{5/2}.$$

Again, fermions need to be vector-like. The Lagrangian of the model is given by:

$$\begin{aligned} \mathscr{L} = & \Big[Y_1 \overline{\chi}_1 P_L L \phi_1 + Y_2 \phi_2^\dagger P_L L \chi_2 + Y_3 \chi_1 S \overline{\chi}_2 + Y_4 e_R \overline{\chi}_1 \phi_2 + Y_5 e_R H^\dagger \chi_1 \\ & + Y_6 e_R e_R \phi_1 + \text{H.c.} \Big] - M_{\chi_1} \overline{\chi}_1 \chi_1 - M_{\chi_2} \overline{\chi}_2 \chi_2 - V_{\text{scalar}}, \end{aligned} \tag{2.8}$$

with the scalar potential:

$$\begin{aligned} V_{\text{scalar}} = & \, m_H^2 H^\dagger H + m_S^2 S^\dagger S + m_{\phi_1}^2 \phi_1^\dagger \phi_1 + m_{\phi_2}^2 \phi_2^\dagger \phi_2 \\ & + \Big[\mu_1 \phi_1^\dagger H^\dagger \phi_2 + \lambda_2 S^\dagger H H H + \lambda_3 \phi_2^\dagger S H H + \lambda_4 \phi_2^\dagger S H^\dagger S + \text{H.c.} \Big] + \frac{1}{2} \lambda_1 (H^\dagger H)^2 \\ & + \frac{1}{2} \lambda_5 (\phi_1^\dagger \phi_1)^2 + \frac{1}{2} \lambda_6 (\phi_2^\dagger \phi_2)^2 + \frac{1}{2} \lambda_7 (S^\dagger S)^2 + \frac{1}{2} \lambda_8 (S^\dagger S^\dagger)(S S) + \lambda_9 (H^\dagger H)(\phi_1^\dagger \phi_1) \\ & + \lambda_{10} (H^\dagger H)(\phi_2^\dagger \phi_2) + \lambda_{11} (H^\dagger H)(S^\dagger S) + \lambda_{12} (\phi_1^\dagger \phi_1)(\phi_2^\dagger \phi_2) + \lambda_{13} (\phi_1^\dagger \phi_1)(S^\dagger S) \\ & + \lambda_{14} (\phi_2^\dagger \phi_2)(S^\dagger S) + \lambda_{15} (H^\dagger \phi_2)(\phi_2^\dagger H) + \lambda_{16} (H^\dagger S)(S^\dagger H) + \lambda_{17} (S^\dagger \phi_2)(\phi_2^\dagger S). \end{aligned} \tag{2.9}$$

Note that the term proportional to λ_2 will induce a non-zero value for the vev of the neutral scalar S, even if m_S^2 is larger than zero. One can thus take either λ_2 or v_S as a free parameter. In our numerical calculation we choose v_S, see below.

3 Low energy constraints

In this section we will discuss non-accelerator constraints on the parameters of our two example models. We consider first neutrino masses and angles and then turn to lepton flavour violating (LFV) decays. The LHC phenomenology is discussed in section 4.

We have implemented both of our example models in SARAH [34, 35]. Using Toolbox [36], the implementation can be used to generate SPheno code [37, 38], for the numerical evaluation of mass spectra and observables, such as LFV decays ($\mu \to e\gamma$, $\mu \to 3e$ etc) calculated using Flavour Kit [39]. The Toolbox subpackage SSP has then be used for our numerical scans.

JHEP01(2018)009

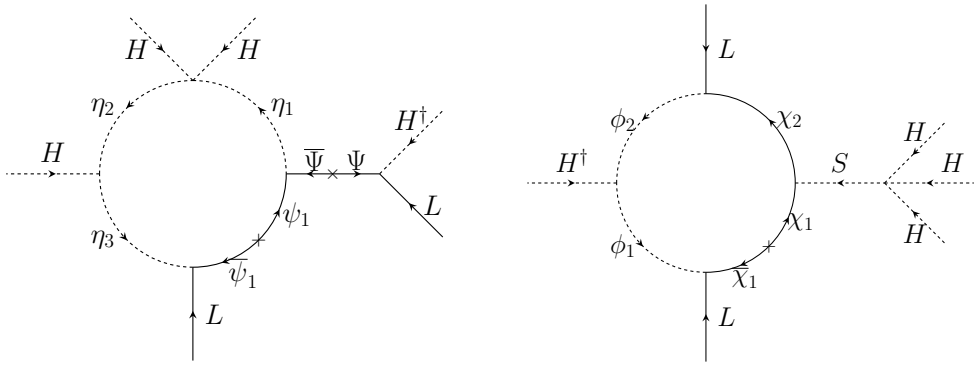

Figure 2. 1-loop neutrino mass diagrams for the triplet model (left) and for the quadruplet model (right). Diagrams are given in the gauge basis. For a discussion see text.

3.1 Neutrino masses

Here we discuss the calculation of neutrino masses in our two example models. We first consider the triplet model, then only briefly summarize the calculation of the quadruplet model, since the calculation is very similar in both cases. Note that SPheno allows to calculate 1-loop corrected masses numerically. We have checked that the description given below agrees very well with the numerical results from SPheno.

The triplet model is described by the Lagrangian given in eq. (2.3) and generates $d = 7$ 1-loop neutrino masses via the diagram shown in figure 2 to the left. Rotating the doubly charged scalars to the mass eigenstate basis, the diagram in figure 2 results in a neutrino mass matrix given by:[5]

$$(m_\nu)_{\alpha\beta} = \frac{1}{16\pi^2}\frac{Y_3 v}{m_\Psi} m_{\psi_1} \sum_i (R_{\eta^{++}})_{1i}(R_{\eta^{++}})_{3i} B_0(0, m^2_{\psi_1}, m^2_{S_i}) \left[(Y_1)_\alpha (Y_2)_\beta + (Y_1)_\beta (Y_2)_\alpha\right]. \tag{3.1}$$

Here $(R_{\eta^{++}})$ is the rotation matrix defined in eq. (2.7) and m_{S_i} are the eigenvalues of eq. (2.5). $B_0(0, m^2_{\psi_1}, m^2_{S_i})$ is a Passarino-Veltman function. In the numerical calculation we have used eq. (3.1) to fit the neutrino masses of the model to neutrino oscillation data. However, in order to have a better understanding of the dependence of eq. (3.1) on the different parameters of the Lagrangian, eq. (2.3), we also give the expression of the neutrino mass matrix in the so-called mass insertion approximation. This approximation consists in replacing the full diagonalization matrices and eigenvalues of the doubly charged scalar mass matrix by their leading order ones. The resulting equation can be written simply as:

$$(m_\nu)_{\alpha\beta} = \mathcal{F} \times \left[(Y_1)_\alpha (Y_2)_\beta + (Y_1)_\beta (Y_2)_\alpha\right], \tag{3.2}$$

[5]Eq. (3.1) is already an approximation: Ψ_0 mixes with the light active neutrinos. So, the total neutral fermion mass matrix is (4,4). However, this mixing should not be too large and is estimated here simply by the factor $\frac{Y_3 v}{m_\Psi}$.

JHEP01(2018)009

where

$$\mathcal{F} = \frac{1}{16\pi^2}\frac{Y_3 v}{m_\Psi}\frac{v^2\lambda_2}{m_{S_2}^2 - m_{S_1}^2}\frac{v\mu_1}{m_{S_3}^2 - m_{S_2}^2}m_{\psi_1} \times\left[\frac{m_{S_1}^2}{m_{\psi_1}^2 - m_{S_1}^2}\ln\left(\frac{m_{S_1}^2}{m_{\psi_1}^2}\right) - \frac{m_{S_2}^2}{m_{\psi_1}^2 - m_{S_2}^2}\ln\left(\frac{m_{S_2}^2}{m_{\psi_1}^2}\right)\right] \tag{3.3}$$

Eq. (3.2) shows that neutrino angles predicted by the model depend on ratios of Yukawa couplings, while the overall mass scale is determined by the prefactor $\mathcal{F}$. The model has the interesting feature that $\det(m_\nu) = 0$. Therefore it can fit only hierarchical neutrino mass spectra (normal or inverse), but not a degenerate spectrum.[6] The eigenvalues of eq. (3.2) are:

$$m_{\nu_{1(3)}} = 0, \quad m_{\nu_{2,3(1,2)}} = \left[\sum_\alpha (Y_1)_\alpha (Y_2)_\alpha \mp \sqrt{\sum_\alpha |(Y_1)_\alpha|^2 \sum_\alpha |(Y_2)_\alpha|^2}\right]\mathcal{F} \tag{3.4}$$

for normal (inverted) hierarchy. From eq. (3.4), one can estimate the constraints from neutrino masses on the size of the Yukawa couplings. In order to reproduce the neutrino mass suggested by atmospheric neutrino oscillations ($m_{\nu_3} \sim 0.05\,\text{eV}$), keeping the mass scale of the new particles $M \sim 1\,\text{TeV}$, the scalar coupling $\lambda_2 \sim 1$ and mass term $\mu \sim 1\,\text{TeV}$, the Yukawa couplings Y_1, Y_2, Y_3 must be set typically to $\mathcal{O}(10^{-2})$. Note, however, that this is only a rough estimate and in our numerical calculations we scan over the free parameters of the model. As discussed in the next subsection, LFV produces upper limits on these Yukawa couplings very roughly of this order.

In our numerical fits to neutrino data, we do not only fit to solar and atmospheric neutrino mass differences, but also to the observed neutrino angles [40]. This is done in the following way. First, we choose all free parameters appearing in the prefactor $\mathcal{F}$. These leaves us with the six free parameters in the two vectors Y_1 and Y_2. Two neutrino masses and three neutrino angles give us five constraints. We arbitrarily choose $(Y_1)_e$ as a free parameter, the remaining five entries are then fixed. Since $\det(m_\nu) = 0$, finding the solutions for those five parameters implies solving coupled quadratic equations, which can be done numerically.

For the quadruplet model we show the neutrino mass diagram in figure 2 to the right. The Lagrangian of this model is given in eq. (2.8). The calculation of the neutrino mass matrix for this model gives:

$$(m_\nu)_{\alpha\beta} = \frac{1}{16\pi^2}\sum_j\sum_i m_{\chi_j^{++}}(R_{S^{++}})_{1i}(R_{S^{++}})_{3i}(R_{\chi^{++}})_{1j}(R_{\chi^{++}})^*_{j2} \times B_0(0, m^2_{\chi_j^{++}}, m^2_{S_i^{++}})\left[(Y_1)_\alpha(Y_2)_\beta + (Y_1)_\beta(Y_2)_\alpha\right]. \tag{3.5}$$

Here $R_{S^{++}}$ and $R_{\chi^{++}}$ are the matrices which diagonalize the doubly charged scalar and fermion mass matrices in the quadruplet model. As in the triplet model, $\det(m_\nu) = 0$. Thus, the fit of neutrino data is analogous to the one described above for the triplet model. Recall, however, that in the numerical calculation we use v_s as a free parameter.

[6] In order to fit also a quasi-degenerate spectrum we would need to include more than one copy of Ψ or/and ψ_1.

JHEP01(2018)009

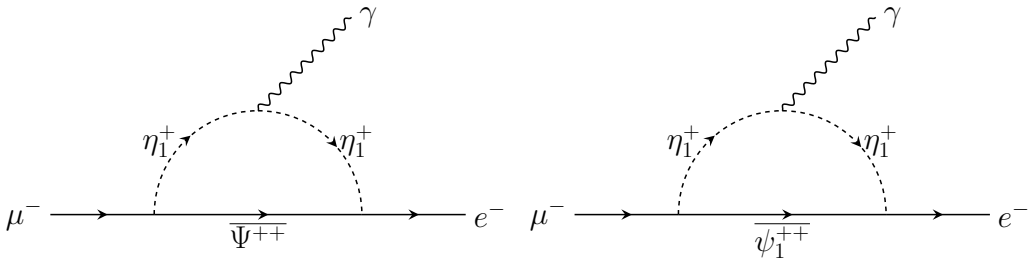

Figure 3. Example diagrams for $\mu \to e\gamma$ in the triplet model, proportional to $(Y_4)_e(Y_4)_\mu$ (left) and $(Y_5)_e(Y_5)_\mu$ (right).

3.2 Lepton flavour violating decays

As is well-known, experimental upper limits on lepton flavour violating decays provide important constraints on TeV-scale extensions of the standard model, see for example [6, 41] and references therein. Flavour Kit [39] implements a large number of observables into SPheno [38]. In the following we will concentrate on $\mu \to e\gamma$, $\mu \to 3e$ and $\mu \to e$ conversion in Ti.

Currently $\mu \to e\gamma$ [42] and $\mu \to 3e$ [43] provide the most stringent constraints. There is also a limit on muon conversion in Ti [44]. However, while there will be only some improvement in the sensitivity in $\mu \to e\gamma$ [45], proposals to improve $\mu \to 3e$ [46] and muon conversion on both Ti [47] and Al [48] exist, which claim current bounds can be improved by 4-6 orders of magnitude. Constraints involving τ's also exist, but are much weaker. Thus, while we routinely calculate constraints also for the τ sector, we will not discuss the results in detail.

Again, let us first discuss the triplet model. The Lagrangian, see eq. (2.3), of the model contains five different Yukawa couplings. We can divide them into two groups: Y_1, Y_2 and Y_3 enter the neutrino mass calculation, while Y_4 and Y_5 are parameters with no relation to m_ν. This implies that for the former, neutrino physics imposes a *lower bound* on certain products of these Yukawas (as a function of the other parameters), while the latter could, in principle, be arbitrarily small.

Consider first the simpler case of Y_4 and Y_5. The diagrams in figure 3 show contributions to $\mu \to e\gamma$ due to these couplings. The current upper limit on $\mathrm{Br}(\mu \to e\gamma)$ then puts a bound on both, Y_4 and Y_5, of roughly $(Y_{4/5})_e(Y_{4/5})_\mu \lesssim 10^{-4}$ for masses of η_1 and Ψ or χ of the order $\mathcal{O}(1)$ TeV.

The fit to neutrino data imposes relations among the parameters Y_1, Y_2 and Y_3, see the discussion in the previous section. Thus, the dependence of LFV decays on these parameters is slightly more subtle. Figure 4 shows results for calculated branching ratios of $\mu \to e\gamma$, $\mu \to 3e$ and $\mu \to e$-conversion in Ti, for several different choices of parameters, as function of Y_3. The horizontal lines show current experimental limits (full lines) and future expected sensitivities (dashed lines). Note that Y_3 has no lepton flavour indices and, thus, by itself can not generate a LFV diagram. Instead, for fixed values of masses and the parameters λ_2 and μ_1, the prefactor $\mathcal{F}$ determining the size of the calculated

JHEP01(2018)009

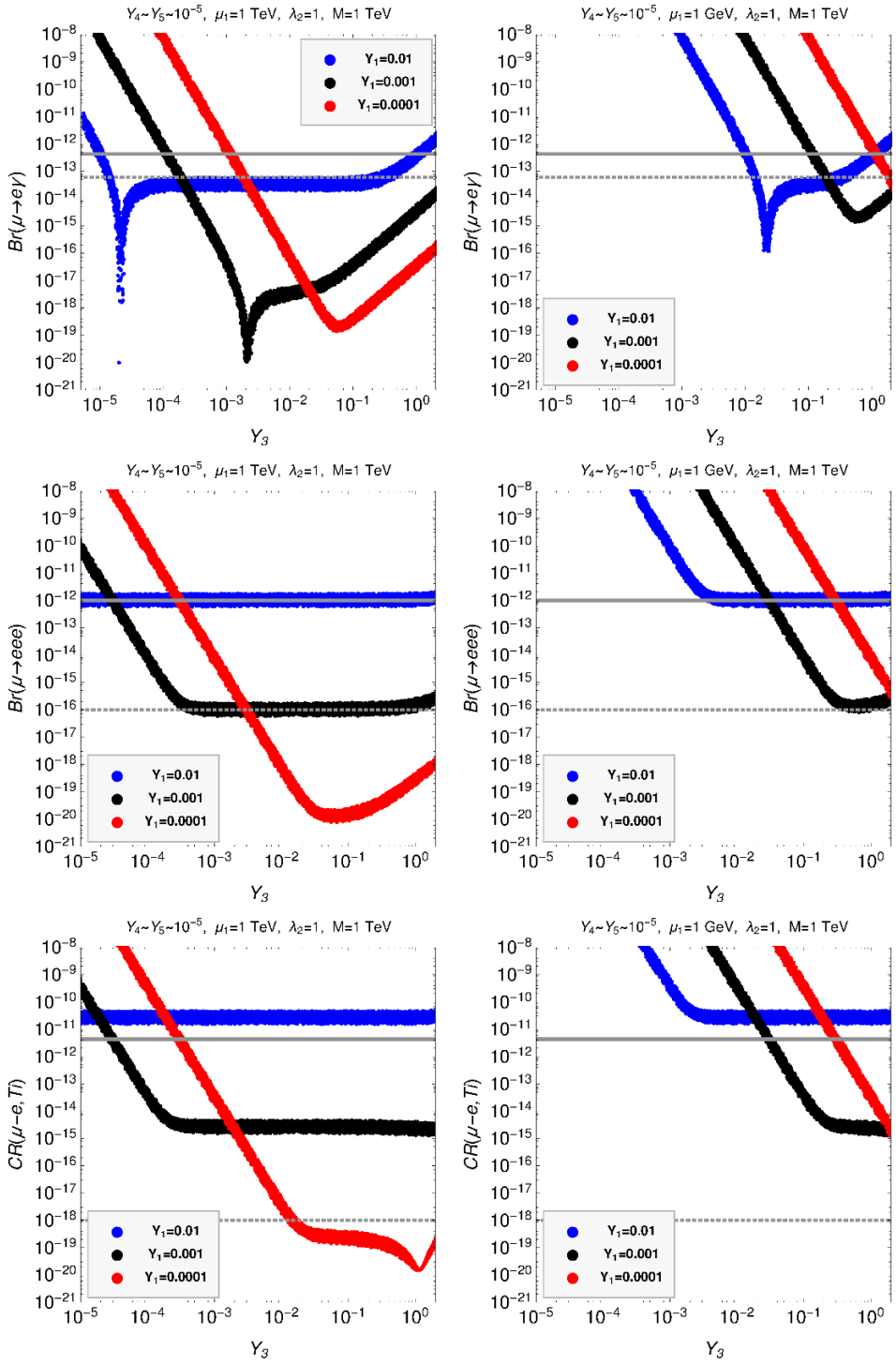

Figure 4. Lepton flavour violating decays calculated in the triplet model. Top panel: $\mathrm{Br}(\mu \to e\gamma)$; middle panel: $\mathrm{Br}(\mu \to 3e)$; bottom: $\mu \to e$ conversion in Ti. Rates are plotted versus the coupling Y_3, for discussion see text. Left row: $\mu_1 = 1\,\mathrm{TeV}$, right row $\mu_1 = 1\,\mathrm{GeV}$. The full (dashed) horizontal lines are the current limits (and future expected sensitivities).

JHEP01(2018)009

neutrino masses, see eq. (3.3), depends linearly on Y_3. Keeping neutrino masses constant while varying Y_3, thus leads to a corresponding change in (the inverse of) $Y_1 \times Y_2$. For this reason, for small values of Y_3 the branching ratios in figure 4 decrease with increasing Y_3. For the largest values of Y_3, diagrams with additional $Y_3 v/m_\Psi$ insertions can become important and branching ratios start to rise again as a function of Y_3. Note that in all calculations in figure 4, we have chosen Y_4 and Y_5 small enough, such that their contribution to the LFV decays is negligible.

Both, Y_1 and Y_2, generate LFV decays. Whether diagrams proportional to $(Y_1)_e(Y_1)_\mu$ or to $(Y_2)_e(Y_2)_\mu$ give the more important contribution to $\mu \to e\gamma$ depends on the (mostly) arbitrary choice of $(Y_1)_e$. In figure 4 we plot results for three different choices of $(Y_1)_e$. For $(Y_1)_e = 10^{-2}$ there is a large range of Y_3, for which $\mu \to e\gamma$ and $\mu \to 3e$ remain constant. In this case, diagrams proportional to $(Y_1)_e(Y_1)_\mu$ dominate the partial width.

We also show in figure 4 two different choices of the parameter μ_1. To the left: $\mu_1 = 1\,\text{TeV}$, to the right $\mu_1 = 1\,\text{GeV}$. Smaller values of μ_1 require again larger values of the Yukawa coupling Y_2, and thus lead to larger LFV decays. While for $\mu_1 = 1\,\text{TeV}$ nearly all points in the parameter space are allowed with current constraints, once $(Y_1)_e$ is smaller than roughly (few) 10^{-3}, for $\mu_1 = 1\,\text{GeV}$ large parts of the parameter space are already ruled out. For $\mu_1 \simeq 10^{-2}\,\text{GeV}$ and masses below 2 TeV there remain already now no valid points in the parameter space which, at the same time, can obey upper limits from $\mu \to e\gamma$ and explain neutrino masses, except in the small regions where different diagrams cancel each other exactly accidentally.

It is worth to mention that for the triplet model the branching ratio of $\mu \to 3e$ is higher than the corresponding of $\mu \to e\gamma$. Naively one would expect the former to be two orders (an order of α_{EM}) lower than the latter. However, $\mu \to e\gamma$ occurs at loop level, while in this model there exists a tree level diagram for $\mu \to 3e$ mediated by a Z^0, due to the mixing between leptons and $\overline{\Psi^+}$, so proportional to $(Y_1)_e(Y_1)_\mu$. Other tree level contributions mediated by doubly-charged scalars are also possible due to this mixing. These are proportional to $(Y_4)_\mu(Y_4)_e(Y_1)_e(Y_1)_e$, so the upper limit given by $\mu \to e\gamma$ is still dominant.

The plots in figure 4 also show the discovery potential of future $\mu \to 3e$ and μ-conversion experiments. In particular, an upper bound on μ conversion of the order 10^{-18} would require both, very small Yukawas (for example: $(Y_1)_e \lesssim 10^{-5}$) and a large value of $\mu_1 \gtrsim 1\,\text{TeV}$ at the same time. All other points in the parameter space of the triplet model (assuming they explain neutrino data) with masses below 2 TeV, should lead to the discovery of μ-conversion. This is an interesting constraint, since such small values of the Yukawa couplings would imply very long lived particles at the LHC. We will come back to this discussion in the next section.

We now turn to a discussion of LFV in the quadruplet model. Similarly to the triplet model, we can divide parameters into two groups: Y_1-Y_3 depend on the neutrino mass fit, while Y_4-Y_6 are unconstrained parameters. Constraints on Y_4 and Y_5 from LFV are very similar to those found in the triplet model. The constraints on Y_6 are somewhat more stringent, $(Y_6)_{\mu e}(Y_6)_{ee} \lesssim 10^{-5}$, since there exists a tree-level diagram via doubly-charged scalar exchange contributing to the decay $\mu \to 3e$.

JHEP01(2018)009

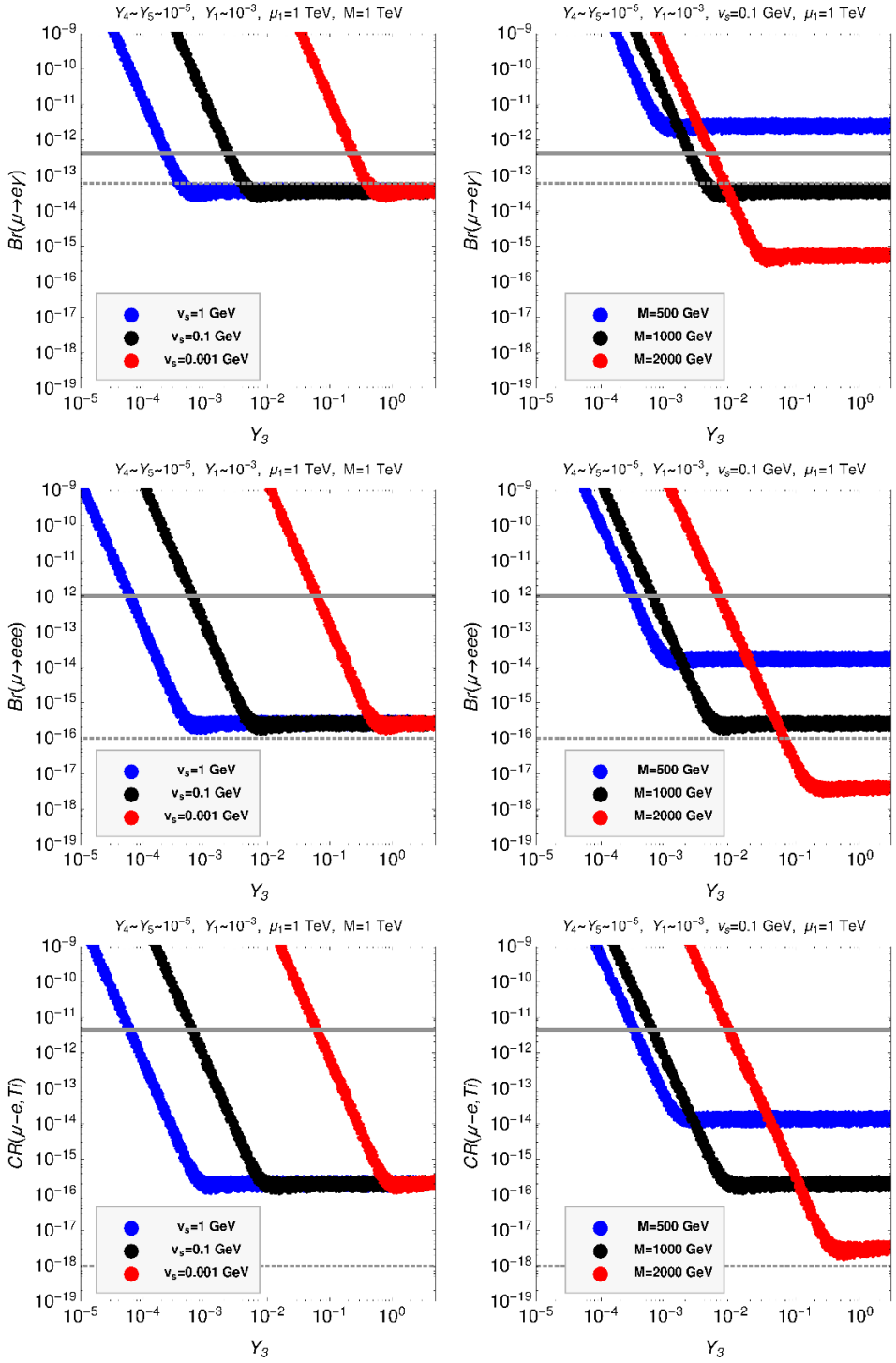

Figure 5. Lepton flavour violating decays calculated in the quadruplet model. Plots to the left show results for different choices of the quadruplet vev v_S, while the ones to the right use different masses for the new scalars and fermions. Here, we assume that all new particles have similar masses of the order indicated in the figure panels.

JHEP01(2018)009

Turning to Y_1-Y_3, figure 5 shows some sample calculations of LFV decays as function of Y_3 in the quadruplet model. The plots to the left show $\mu \to e\gamma$, $\mu \to 3e$ and μ-conversion in Ti, for several different choices of the quadruplet vev v_S. Smaller values of v_S need larger values of the Yukawa couplings Y_2 for constant neutrino masses. Thus, LFV decays are larger at the same values of Y_3 for smaller values of v_S. The plots on the right of figure 5 show the same LFV decays, for a fixed value of $v_S = 0.1\,\text{GeV}$, but different values of the new scalar and fermion masses. As simplification in this plot we assume that all new scalars and fermions have roughly the same mass, M, as indicated in the plot panels. Larger values of masses lead to smaller LFV decay widths, as expected. As also is the case for the triplet model, future bounds from $\mu \to 3e$ and $\mu \to e$-conversion will test most of the relevant parameter space of the quadruplet model up to masses of order 2 TeV.

In fact, even for masses as large as 2 TeV, non-observation of $\mu \to e$ conversion would put an interesting lower limit on the value of v_S, which we roughly estimate to be around $v_S = 0.1\,\text{GeV}$. Note that there is an upper limit on v_S from the SM ρ parameter of the order of $v_S \lesssim 2.5\,\text{GeV}$ [10].

In summary, the non-observation of LFV decays can be used to put upper bounds on the Yukawa couplings of our models. At the same time the observed neutrino masses require lower bounds on these Yukawa couplings and the combination of both constraints result in a very restricted range of allowed parameters. We have shown this explicitly only for our two example models, but the same should be true for any of the possible (genuine) $d = 7$ 1-loop models.

4 Phenomenology at the LHC

4.1 Constraints from LHC searches

We have calculated the production cross sections for the different scalars and fermions of our example models using MadGraph [49]. Pair production is usually calculated via s-channel photon and Z^0 exchange, while associated production, such as $\eta^{--}\eta^{+++}$, proceeds via W^+ diagrams. However, as pointed out in [30], for large masses the pair production cross section of charged particles via photon-photon fusion can give the dominant contribution to the cross section, despite the small photon density in the proton. In our calculation we use the NNPDF23_nlo_as_0119 parton distribution function, which contains NLO corrections, necessary for inclusion of the photon-photon fusion contributions. We have checked numerically and find that at the largest masses cross sections can be enhanced up to one order of magnitude for multiply charged particles. For this reason we concentrate on pair production of particles in the following. Note, however, that for lower masses (up to roughly 1 TeV), associated production is large enough to produce additional signals, not discussed here.

Results for the cross sections are shown in figure 6 for $\sqrt{s} = 13\,\text{TeV}$. To the left we show results for scalars, to the right the cross sections for fermions. The scalar cross sections (to the left) where calculated for the scalars of the triplet model. The fermion cross section (to the right) correspond to the fermions of the quadruplet model. The underlying Lagrangian parameters were chosen such, that the corresponding gauge states (index shown in the

JHEP01(2018)009

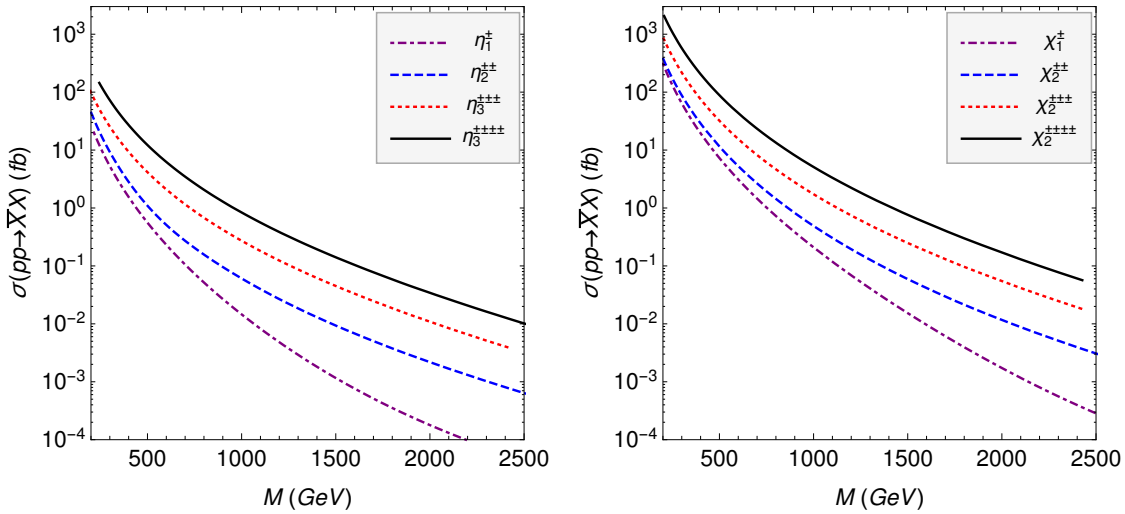

Figure 6. Pair production cross sections for the different scalars (left) and fermions (right) of the two example models. For discussion see text.

figure) are the lightest mass eigenstate of the corresponding charge. Cross sections do also depend, to some extent, on the hypercharge of the particle. However, since photon-fusion dominates the cross section at large values of the masses, all mass eigenstates with the same electric charge have similar cross sections. We therefore do not repeat those plots for all particles in our models.

For the quadruply charged particles of the models cross sections larger than 10^{-2} fb are obtained, even for masses up to 2.5 TeV. Note that at the largest value of masses pair production cross section ratios for differently charged particles simply scale as the ratio of the charges to the 4th power. We will come back to this in the discussion of the LNV signals in the next subsection.

A number of different LHC searches can be used to set limits on the various particles of our example models. The simplest search, and currently the most stringent LHC limit for our models, comes from a recent ATLAS search for doubly charged particles decaying to either $e^{\pm}e^{\pm}$, $e^{\pm}\mu^{\pm}$ or $\mu^{\pm}\mu^{\pm}$ final states [27]. Results of our calculation, compared to the experimental limit are shown in figure 7 for the $\mu^{\pm}\mu^{\pm}$ final state.

The two-body decay with of the doubly charged scalar η_1^{++} is approximately given by:

$$\Gamma(\eta_1^{++} \to l_\alpha^+ l_\beta^+) \simeq \frac{1}{8\pi}\left(\frac{v}{m_\Psi}\right)^2 \left[(Y_4)_\alpha (Y_1)_\beta + (Y_4)_\beta (Y_1)_\alpha\right]^2 m_{\eta_1^{++}} \tag{4.1}$$

Since the Yukawa coupling Y_4 does not enter the neutrino mass calculation, the exact value and flavour composition of this decay can not be predicted. However, Y_1 enters our neutrino mass fit. The observed large neutrino angles require that all entries in the vector Y_1 are different from zero and of similar order. Typically, from the fit we find numerically ratios in the range $(Y_1)_e : (Y_1)_\mu : (Y_1)_\tau \sim ([1/4, 1/2] : [1, 3] : 1)$, but the exact ratios depend on the allowed range of neutrino angles. Scanning over the allowed neutrino parameters then leads to a variation of the branching ratios of the η_1^{++} into the different lepton generations. This explains the spread of the numerically calculated points in figure 7. Combined with the

JHEP01(2018)009

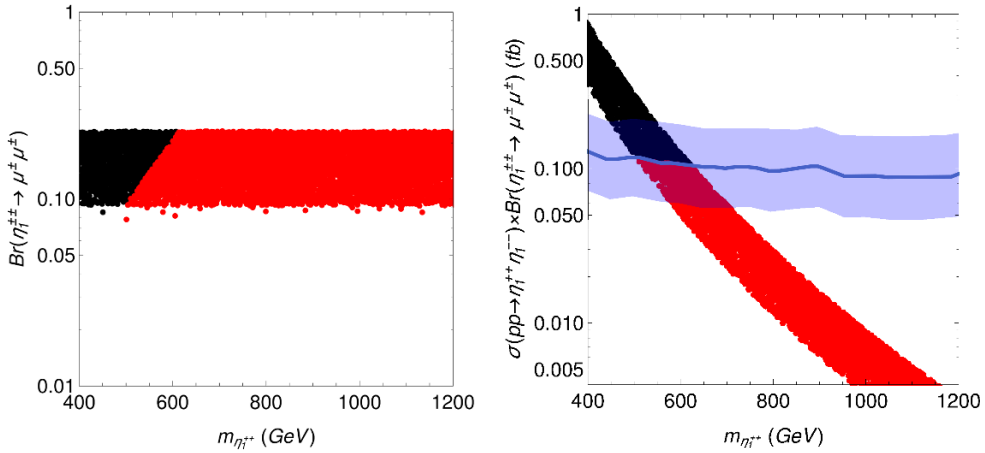

Figure 7. To the left, an example of a branching ratio of a doubly charged scalar to two leptons. The spread of the value of the branching ratio is due to the fact that points in our calculation are obtained scanning over the allowed neutrino angles (3σ). To the right, the current constraints on doubly charged scalars, using the recent search by ATLAS [27]. The blue line is the limit quoted in [27], the light blue region the 95 % c.l. region. Red points are allowed by this search, black points are excluded.

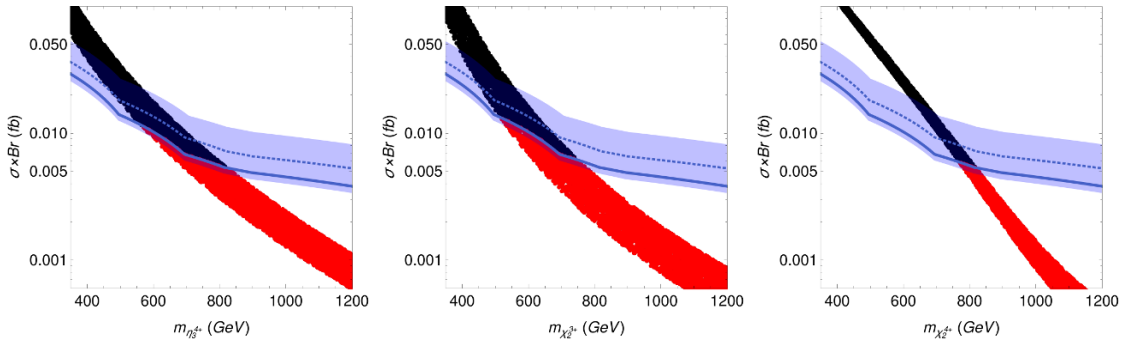

Figure 8. Current constraints on charged scalars and fermions using the multi-lepton search [31]. Points are our numerical results, the bands are experimental limits, see also figure 7.

experimental limit from ATLAS, lower mass limits in the range of (500–650) GeV result. Note that in this plot, we allow all three neutrino angles to float within the 3 σ regions of the global fit [40].

The CMS collaboration has recently published a search based on multi-lepton final states [31]. The original motivation for this search is the expectation that the fermions of the seesaw type-III lead to final states containing multiple charged leptons and missing momentum. For example, $\Sigma^\pm\Sigma^0 \to W^\pm\nu W^\pm l^\mp$ from the associated production of the fermionic triplet $\Sigma = (\Sigma^+, \Sigma^0, \Sigma^-)$. The analysis [31] requires than at least three charged leptons plus missing energy and takes into account both, electrons and muons.

In our models, these final states can occur in various decay chains. Consider for example χ_2^{4+}. Once produced, it can decay into a $\chi_1^{3+} + W^+$, which further decays to a doubly charged scalar and l^+. The doubly charged scalar decays to either leptons or W's. The missing energy is then produced in the leptonic decays of the W's. Here, all

JHEP01(2018)009

Multiplicity	LNV Signal	Particles	Model	Mass range
4 (6)	$l^\pm l^\pm + W^\mp W^\mp$	$S^{\pm\pm}$, $\phi_1^{\pm\pm}$, $\phi_2^{\pm\pm}$	Q	$m < 1.4\,\text{TeV}$
6 (8)	$l^\pm l^\pm l^\pm + W^\mp W^\mp l^\mp$	χ_2^{3+}	Q	$m < 2.6$ TeV
6 (10)	$l^\pm l^\pm W^\pm + W^\mp W^\mp W^\mp$	S^{3+}, ϕ_2^{3+}	Q	$m < 2.0$ TeV
8 (10)	$l^\pm l^\pm l^\pm l^\pm + l^\mp l^\mp W^\mp W^\mp$	η_3^{4+}	T	$m < 2.5\,\text{TeV}$
8 (12)	$l^\pm W^\pm W^\pm W^\pm + l^\mp l^\mp l^\mp W^\mp$	χ_2^{4+}	Q	$m < 3.2\,\text{TeV}$
8 (14)	$l^\pm l^\pm W^\pm W^\pm + W^\mp W^\mp W^\mp W^\mp$	—	—	

Table 1. List of "symmetric" LNV final states in $d = 7$ models. The first column counts the number of final state particles, the second column gives the LNV signal. The multiplicity is given twice, the value without the bracket gives the number counting W's, while the number in brackets counts each W as two jets. This is done, since only the hadronic decays of the W can be used for establishing LNV, see text. Here, we have separated the total final state into the two sets of particles, coming from the pair produced states listed in column 3. The invariant masses of the quoted subsystems should peak at the mass of the particle quoted in column 3. Column four gives the model in which this signal could be found. The last column gives our simple estimate for the mass range, which can be probed at the LHC with $\mathcal{L} \simeq 300/\text{fb}$. For a discussion see text.

intermediate particles can be either on-shell or off-shell, depending on the unknown mass hierarchies. Constraints can then be derived from the results of [31], scanning over the allowed ranges of the branching ratios, which lead to a least three charged leptons plus at least one W in the final state.

In figure 8 we show results of this procedure for the examples of η_3^{4+}, χ_2^{3+} and χ_2^{4+}. The lower limits, derived from this exercise, have a rather large uncertainty, due to the unknown branching ratios. For example, the lower mass limit for η_3^{4+} is in the range of (550–850) GeV. Note that η_3^{4+} could decay, in principle to four charged leptons with a branching ratio close to 100 %. The final state from pair production of η_3^{4+} would then contain eight charged leptons and missing momentum would appear only from the decays of the τ's. In this case, our simple-minded recasting of the multi-lepton search [31] ceases to be valid and the lower limit on the mass of η_3^{4+}, mentioned above does not apply. As figure 8 shows, the lower limit on the mass of χ_2^{4+} is more stringent than the one for η_3^{4+}. This simply reflects the larger production cross sections for fermions, compare to figure 6.

4.2 New LNV searches

We now turn to a discussion of possible LNV signals at the LHC. Table 1 shows examples of different LNV final states from pair production of scalars or fermions in the two models under consideration. This list is not complete since (a) associated producion of particles is not considered; (b) the table gives only "symmetric" LNV states, see below, and (c) we do not give LNV final states with neutrinos, since such states do not allow to establish LNV experimentally.

The table gives in column 1 the multiplicity of the final state and in column 2 the LNV signal. The multiplicity in column 1 is given twice, once counting directly the number of leptons and W's (value without bracket) and second, counting each W as two jets in the

JHEP01(2018)009

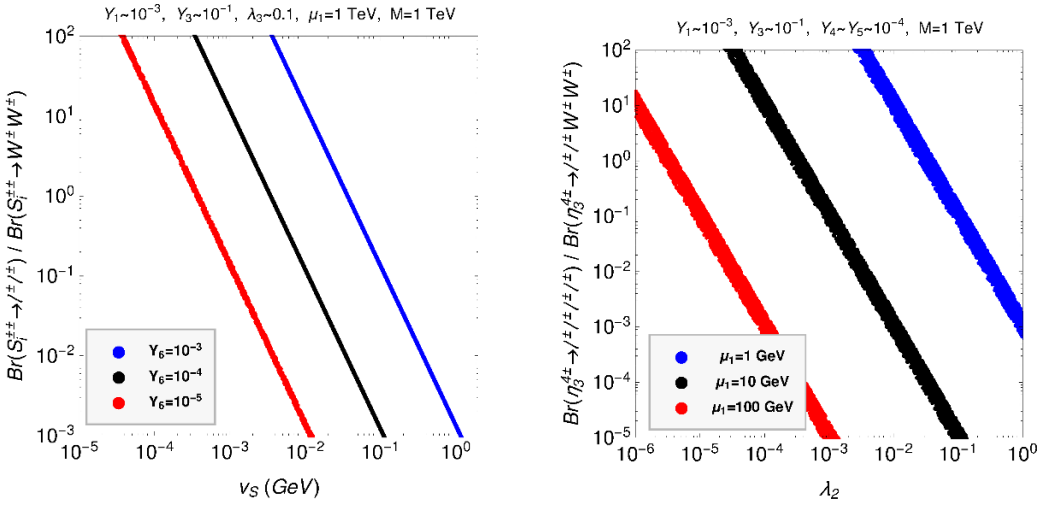

Figure 9. To the left: ratio of branching ratios of the doubly charged scalar, S_1^{++} decaying to $l^\pm l^\pm$ divided by $W^\pm W^\pm$ as a function of v_S for some fixed choice of the other model parameters and three different values of Y_6. This plot assumes that the lightest doubly charged scalar S_1^{++} is mostly the gauge state S^{++}. Results for the other cases are qualitatively very similar and thus not repeated. To the right: ratio of branching ratios for η_3^{4+} decays. As in the case of S_1^{++}, LNV will be observable only if this ratio is of order $\mathcal{O}(1)$.

final state (number in bracket). We stress again that the leptonic decays of the W can be used in searches to derive lower mass limits on exotic particles, but can not be used to *establish* LNV experimentally. This is because the neutrinos from the leptonic W decays show up only as missing energy, i.e. their lepton number can never be tagged. In the following, we will discuss final states as leptons plus W, but one should always bear in mind that we assume the W to decay hadronically.

In the 2nd column, the two possible final states from the decay of the particle given in column 3 are given seperately. The invariant masses of both separate subsystems in column 2, should therefore give peaks in the mass of the particle in column 3.

Particles in column 3 are quoted as gauge eigenstates. However, scalars in our models are, in general, admixtures of different gauge eigenstates. Consider, for example, the simplest final state $l^\pm l^\pm + W^\mp W^\mp$. $\phi_1^{\pm\pm}$ can decay to $l^\pm l^\pm$, via the coupling Y_6, while $S^{\pm\pm}$ can decay to $W^\pm W^\pm$ via the induced vev v_S (or, equivalently proportional to λ_2). The doubly charged scalars mix via the entries in the mass matrices proportional to μ_1, λ_3 (and λ_4), see eq. (2.9). Whether the lightest doubly charged mass eigenstate is mostly ϕ_1, ϕ_2 or S depends on the choice of parameters, but the results are qualitatively very similar in all cases. We therefore show in figure 9 only the results for the case where S_1^{++} is mostly S.

Figure 9 (left) shows the ratio of branching ratios of the doubly charged scalar, S_1^{++} decaying to $l^\pm l^\pm$ divided by the decay to $W^\pm W^\pm$ as a function of v_S for some fixed choice of the other model parameters and three different values of Y_6. Observation of LNV is only possible, if $\Gamma(S_i^{\pm\pm} \to l^\pm l^\pm)$ is of similar order than $\Gamma(S_i^{\pm\pm} \to W^\pm W^\pm)$, since both final states are needed to establish that LNV is indeed taking place. One can see from the figure that equality of partial widths is possible for different choices of parameters. However, since

JHEP01(2018)009

the decay to two charged leptons is proportional to (the square of) a Yukawa coupling that is not fixed by our neutrino mass fit, the relative ratio of branching ratios can not be predicted from current data.

Similarly, also for all other decays to LNV final states, the two competing final states have to have similar branching ratios. Figure 9 to the right show results for the decay of η_3^{4+} of the triplet model. Depending on the parameter μ_1 equality of branching ratio can occur in a large range of values of the parameter λ_2. Note that the rate of LNV final states is not suppressed by the smallness of neutrino masses. Neutrino masses require the product of $\mathcal{F} \times Y_1 Y_2$ to be small, see eq. (3.2). For a fixed neutrino mass, smaller values of $\mu_1 \lambda_2$ require larger Yukawa couplings $Y_1 Y_2 Y_3$. Depending on the ratio between $\mu_1 \lambda_2$ and $Y_1 Y_2 Y_3$, either the final state $4l$ or the final state $2l + 2W$ can dominate. Whether LNV rates are observable, therefore, does not depend so much on absolute values of some (supposedly small) parameters, but on certain ratios of these parameters.

Table 1 is ordered with respect to increasing multiplicity of the final state. Note that, as discussed in the last subsection, cross sections at the LHC increase with electric charge and decrease (strongly) with increasing mass. Which of the possible signals has the largest rate, can not be predicted because of the unknown mass spectrum. However, if the different members of the scalar (or fermion) multiplets have similar masses, final states with larger multiplicities have actually larger rates at the LHC. Since large multiplicity final states also have lower backgrounds, searches for such states should give stronger bounds.

The last column in table 1 gives our estimate for the reach of the LHC. The numbers for the mass reach quoted in that column are simply based on the cross section calculation, discussed in the last subsection. We assume here that in particular for the high multiplicity final states SM backgrounds are very low (order of one event or less). Then we simply take the cross section for which 3 events for a luminosity of 300 fb^{-1} are produced as the approximate limit, that maybe achieved in a dedicated search. In fact, with supposedly no backgrounds even slightly lower masses than those quoted in the table would lead to 5 or more events, which maybe sufficient for a discovery.

However, we need to mention that our calculation, using MadGraph, calculates the cross-sections at leading order only. Also our calculation does not include any cuts and thus, should be taken only as a rough estimate. Thus the numbers in the table should probably come with an uncertainty of the order of (100–150) GeV or so for the larger multiplicity states. On the other hand, for the simpler signal $pp \to l^+ l^+ W^- W^-$, the number given in the table should be taken with a grain of salt. Currently for dilepton searches with luminosity of 36 fb^{-1} there are no background events in the bins above 1 TeV in the invariant mass distribution $m(ll)$, see [27]. This in turns implies for a luminosity of 300 fb^{-1} in the most pessimistic case an upper limit of roughly 8 background events for the signal $pp \to l^+ l^+ W^- W^-$. Our estimate of 3 signal events would then correspond only a 1 σ c.l. limit.

We mention that the final state with 2 l and 6 W's and LNV signals with 10 or more particles are also possible in $d = 7$ 1-loop models, but do not occur within our two example models. This is simply due to the fact that scalars or fermions with 5 units of charge are needed for such states. Thus, such signals can appear in versions of the $d = 7$ 1-loop type

JHEP01(2018)009

models, that include larger $\mathrm{SU}(2)_L$ representations, such as quintuplets, or with particles with a larger hypercharge.

Finally, the table considers only "symmetric" LNV final states. Here, by symmetric we define that both branches of the decay contain the same number of final states particles. For example, for the quadruplet model, we have included the LNV signal with "symmetric" final states $pp \to \chi_2^{3+}\chi_2^{3-}, \chi_2^{3+} \to l^+l^+l^+, \chi_2^{3-} \to W^-W^-l^-$, but we have not considered the possible LNV signal with asymmetric final states $pp \to \chi_2^{++}\chi_2^{--}, \chi_2^{++} \to l^+W^+, \chi_2^{--} \to W^-W^-W^-l^+$. The reason for this choice is simply that we consider "asymmetric" LNV signals, although in principle possible, are less likely to occur. This can be understood simply from phase space considerations: a two-body final state has a prefactor of $\frac{1}{8\pi}$ in the partial width, while a four-body phase space is smaller by a factor $3072\pi^4$. Naturally one than expects that the ratio of branching ratios for these asymmetric cases is never close to one, unless there is a corresponding hierarchy in the couplings involved.

Decay widths for the lightest particle in our models are often very small numerically. This opens up the possibility that some particle decays might occur with a displaced vertex. Displaced vertices are more likely to occur in the triplet model, so we concentrate in our discussion on this case. The two-body decay width of η_1^{++} is estimated in eq. (4.1). For the decay of η_3^{3+}, assuming η_3^{3+} is the lightest particle, one can estimate:

$$\Gamma(\eta_3^{+++} \to W^+l^+l^+) \sim \frac{1}{32\pi^2}\left(\frac{\mu_1}{m^2_{\eta_2^{++}}}\right)^2 \frac{m^3_{\eta_3^{++}}}{m_{\eta_1^{++}}}\theta^2_{\eta_1\eta_2}\Gamma(\eta_1^{++} \to l^+l^+). \tag{4.2}$$

Here, $\theta_{\eta_1\eta_2}$ is the mixing angle between the states η_1 and η_2. Eq. (4.2) contains three parameters related to the smallness of the observed neutrino masses: μ_1, $\theta_{\eta_1\eta_2}$ and Y_1. Assuming all mass parameters roughly equal $\mu_1 \simeq m_{\eta_3^{++}} \simeq m_{\eta_2^{++}} \simeq m_{\eta_1^{++}} = M$ this leads to the estimate:

$$L_0(\eta_3^{3+} \to W^+l^+l^+) \sim 0.3\left(\frac{10^{-1}}{\theta_{\eta_1\eta_2}}\right)^2\left(\frac{10^{-2}}{|Y_1|}\right)^2\left(\frac{10^{-2}}{|Y_4|}\right)^2\left(\frac{m_\psi}{\mathrm{TeV}}\right)^2\left(\frac{\mathrm{TeV}}{M}\right)\mathrm{mm}. \tag{4.3}$$

Here, the choice for the Yukawa couplings being order 10^{-2} is motivated by the upper limits on the CLFV branching ratios, discussed in the last section. Eq. (4.3) represents only a very rough estimate, but it is worth pointing out that more stringent upper limits from charged LFV would result in smaller values for the Yukawa couplings, leading to correspondingly large decay lengths. Note also that smaller values of μ_1 would lead to quadratically large lengths. Eq. (4.3) shows that displaced vertices can occur easily in the decay of η_3^{3+}.

Similarly, one can estimate roughly the order of magnitude of the decay length for η_3^{4+}. The result is:

$$L_0(\eta_3^{4+} \to W^+W^+l^+l^+) \sim 4\left(\frac{1}{\lambda_2}\right)^2\left(\frac{10^{-2}}{|Y_1|}\right)^2\left(\frac{10^{-2}}{|Y_4|}\right)^2\left(\frac{m_\psi}{\mathrm{TeV}}\right)^2\left(\frac{\mathrm{TeV}}{M}\right)\mathrm{cm}. \tag{4.4}$$

The width of η_3^{4+} is smaller than the corresponding one for η_3^{3+} due to the phase space suppression for a 4-body final state. Eq. (4.4) shows that within the triplet model a displaced vertex for the decay of η_3^{4+} is actually expected.

JHEP01(2018)009

5 Discussion and conclusions

In this paper we have discussed the phenomenology of $d = 7$ 1-loop neutrino mass models. Models in this class are far from the simplest variants of BSM models that can fit existing neutrino data, but are interesting in their own right, since they predict that new physics must exist below roughly 2 TeV. If neutrino masses were indeed generated by one of the models in this class, one can thus expect that the LHC will find signatures of new resonances. Searches for doubly charged scalars and multi-lepton final states already put some bounds on these models. However, for the most interesting aspect of $d = 7$ 1-loop models, namely lepton number violating final states, no LHC search exists so far. In particular, final states with large multiplicites are predicted to occur (multiple W and multiple leptons) for which we expect standard model backgrounds to be negligible.

In our discussion, we have limited ourselves to just two simple example models. Our motivation to do so is that all $d = 7$ 1-loop neutrino mass models, which are genuine in the sense that they give the leading contribution to neutrino mass without invoking new symmetries, predict similar LHC signals. The two models which we considered have either a $\mathrm{SU}(2)_L$ triplet or a quadruplet as the largest representations. Other $d = 7$ models will contain even larger $\mathrm{SU}(2)_L$ multiplets and thus also particles with multiple electric charges, to which very similar constraints than those analysed here will apply.

Finally, we mention that there exist variants of $d = 7$ 1-loop models, in which the internal scalars and fermions carry non-trivial colour charges. These variants are not fully covered by our analysis. While the neutrino mass fit and the constraints from LFV searches will be qualitatively very similar to what we have discussed here, additional color factors in the calculations will lead to some quantitative changes. The resulting bounds will, in general be somewhat more stringent than the numbers we give in this paper. More important, however, are the changes in the LHC phenomenology. For example, in the colour-singlet models, which we analyzed in this paper, the lightest doubly charged scalar will decay to two charged leptons. In the coloured variants of the model, the corresponding lightest scalar will behave like a leptoquark, decaying to $l + j$, instead. Thus, different LHC searches will apply to the coloured $d = 7$ models. More interesting, however, is that for coloured models also the LNV final states, which we discussed, will change, since at the end of the decay chain instead of two charged lepton, one lepton plus jet will appear. Although this variety of signals will be interesting in their own rights, we have concentraged here on the colour singlet variants of the model, because di-leptons are cleaner (and thus more easy to probe) in the challenging experimental environment that is the LHC.

Acknowledgments

This work was supported by the Spanish MICINN grants FPA2014-58183-P, SEV-2014-0398, FPU15/03158 (MECD) and PROMETEOII/2014/084 (Generalitat Valenciana). J.C.H. is supported by Chile grants Fondecyt No. 1161463, Conicyt PIA/ACT 1406 and Basal FB0821.

JHEP01(2018)009

Open Access. This article is distributed under the terms of the Creative Commons Attribution License (CC-BY 4.0), which permits any use, distribution and reproduction in any medium, provided the original author(s) and source are credited.

References

[1] F.F. Deppisch, M. Hirsch and H. Pas, *Neutrinoless double beta decay and physics beyond the standard model*, *J. Phys.* **G 39** (2012) 124007 [arXiv:1208.0727] [INSPIRE].

[2] F.T. Avignone, III, S.R. Elliott and J. Engel, *Double beta decay, Majorana neutrinos and neutrino mass*, *Rev. Mod. Phys.* **80** (2008) 481 [arXiv:0708.1033] [INSPIRE].

[3] P. Minkowski, $\mu \to e\gamma$ *at a rate of one out of* 10^9 *muon decays?*, *Phys. Lett.* **67B** (1977) 421 [INSPIRE].

[4] T. Yanagida, *Horizontal symmetry and masses of neutrinos*, *Conf. Proc.* **C 7902131** (1979) 95 [INSPIRE].

[5] R.N. Mohapatra and G. Senjanović, *Neutrino mass and spontaneous parity violation*, *Phys. Rev. Lett.* **44** (1980) 912 [INSPIRE].

[6] Y. Cai, J. Herrero-García, M.A. Schmidt, A. Vicente and R.R. Volkas, *From the trees to the forest: a review of radiative neutrino mass models*, *Front. in Phys.* **5** (2017) 63 [arXiv:1706.08524] [INSPIRE].

[7] F. Bonnet, M. Hirsch, T. Ota and W. Winter, *Systematic study of the* $D = 5$ *Weinberg operator at one-loop order*, *JHEP* **07** (2012) 153 [arXiv:1204.5862] [INSPIRE].

[8] D. Aristizabal Sierra, A. Degee, L. Dorame and M. Hirsch, *Systematic classification of two-loop realizations of the Weinberg operator*, *JHEP* **03** (2015) 040 [arXiv:1411.7038] [INSPIRE].

[9] F. Bonnet, D. Hernandez, T. Ota and W. Winter, *Neutrino masses from higher than* $D = 5$ *effective operators*, *JHEP* **10** (2009) 076 [arXiv:0907.3143] [INSPIRE].

[10] K.S. Babu, S. Nandi and Z. Tavartkiladze, *New mechanism for neutrino mass generation and triply charged Higgs bosons at the LHC*, *Phys. Rev.* **D 80** (2009) 071702 [arXiv:0905.2710] [INSPIRE].

[11] R. Cepedello, M. Hirsch and J.C. Helo, *Loop neutrino masses from* $d = 7$ *operator*, *JHEP* **07** (2017) 079 [arXiv:1705.01489] [INSPIRE].

[12] J.C. Helo, M. Hirsch, S.G. Kovalenko and H. Pas, *Neutrinoless double beta decay and lepton number violation at the LHC*, *Phys. Rev.* **D 88** (2013) 011901 [arXiv:1303.0899] [INSPIRE].

[13] J.C. Helo, M. Hirsch, H. Päs and S.G. Kovalenko, *Short-range mechanisms of neutrinoless double beta decay at the LHC*, *Phys. Rev.* **D 88** (2013) 073011 [arXiv:1307.4849] [INSPIRE].

[14] W.-Y. Keung and G. Senjanović, *Majorana neutrinos and the production of the right-handed charged gauge boson*, *Phys. Rev. Lett.* **50** (1983) 1427 [INSPIRE].

[15] CMS collaboration, *Search for heavy neutrinos and W bosons with right handed couplings in proton-proton collisions at* $\sqrt{s} = 13$ *TeV*, CMS-PAS-EXO-16-045 (2016).

[16] CMS collaboration, *Search for heavy neutrinos and W bosons with right-handed couplings in proton-proton collisions at* $\sqrt{s} = 8$ *TeV*, *Eur. Phys. J.* **C 74** (2014) 3149 [arXiv:1407.3683] [INSPIRE].

JHEP01(2018)009

[17] CMS collaboration, *Search for third-generation scalar leptoquarks and heavy right-handed neutrinos in final states with two tau leptons and two jets in proton-proton collisions at* $\sqrt{s} = 13$ *TeV*, *JHEP* **07** (2017) 121 [arXiv:1703.03995] [INSPIRE].

[18] CMS collaboration, *Search for heavy Majorana neutrinos in* $e^{\pm}e^{\pm}$ *+ jets and* $e^{\pm}$ $\mu^{\pm}$ *+ jets events in proton-proton collisions at* $\sqrt{s} = 8$ *TeV*, *JHEP* **04** (2016) 169 [arXiv:1603.02248] [INSPIRE].

[19] ATLAS collaboration, *Search for heavy Majorana neutrinos with the ATLAS detector in pp collisions at* $\sqrt{s} = 8$ *TeV*, *JHEP* **07** (2015) 162 [arXiv:1506.06020] [INSPIRE].

[20] J. Schechter and J.W.F. Valle, *Neutrino masses in* SU(2) × U(1) *theories*, *Phys. Rev.* **D 22** (1980) 2227 [INSPIRE].

[21] G. Azuelos, K. Benslama and J. Ferland, *Prospects for the search for a doubly-charged Higgs in the left-right symmetric model with ATLAS*, *J. Phys.* **G 32** (2006) 73 [hep-ph/0503096] [INSPIRE].

[22] P. Fileviez Perez, T. Han, G.-y. Huang, T. Li and K. Wang, *Neutrino masses and the CERN LHC: testing type II seesaw*, *Phys. Rev.* **D 78** (2008) 015018 [arXiv:0805.3536] [INSPIRE].

[23] A. Melfo, M. Nemevšek, F. Nesti, G. Senjanović and Y. Zhang, *Type II seesaw at LHC: the roadmap*, *Phys. Rev.* **D 85** (2012) 055018 [arXiv:1108.4416] [INSPIRE].

[24] K.S. Babu and S. Jana, *Probing doubly charged Higgs bosons at the LHC through photon initiated processes*, *Phys. Rev.* **D 95** (2017) 055020 [arXiv:1612.09224] [INSPIRE].

[25] ATLAS collaboration, *Search for anomalous production of prompt same-sign lepton pairs and pair-produced doubly charged Higgs bosons with* $\sqrt{s} = 8$ *TeV pp collisions using the ATLAS detector*, *JHEP* **03** (2015) 041 [arXiv:1412.0237] [INSPIRE].

[26] ATLAS collaboration, *Search for doubly-charged Higgs bosons in same-charge electron pair final states using proton-proton collisions at* $\sqrt{s} = 13$ *TeV with the ATLAS detector*, ATLAS-CONF-2016-051 (2016).

[27] ATLAS collaboration, *Search for doubly-charged Higgs boson production in multi-lepton final states with the ATLAS detector using proton-proton collisions at* $\sqrt{s} = 13$ *TeV*, ATLAS-CONF-2017-053 (2017).

[28] CMS collaboration, *Search for a doubly-charged Higgs boson with* $\sqrt{s} = 8$ TeV *pp collisions at the CMS experiment*, CMS-PAS-HIG-14-039 (2014).

[29] F. del Aguila, M. Chala, A. Santamaria and J. Wudka, *Discriminating between lepton number violating scalars using events with four and three charged leptons at the LHC*, *Phys. Lett.* **B 725** (2013) 310 [arXiv:1305.3904] [INSPIRE].

[30] K. Ghosh, S. Jana and S. Nandi, *Neutrino mass generation at TeV scale and new physics signatures from charged Higgs at the LHC for photon initiated processes*, arXiv:1705.01121 [INSPIRE].

[31] CMS collaboration, *Search for evidence of the type-III seesaw mechanism in multilepton final states in proton-proton collisions at* $\sqrt{s} = 13$ *TeV*, *Phys. Rev. Lett.* **119** (2017) 221802 [arXiv:1708.07962] [INSPIRE].

[32] S. Weinberg, *Baryon and lepton nonconserving processes*, *Phys. Rev. Lett.* **43** (1979) 1566 [INSPIRE].

JHEP01(2018)009

[33] E. Ma, *Pathways to naturally small neutrino masses*, *Phys. Rev. Lett.* **81** (1998) 1171 [hep-ph/9805219] [INSPIRE].

[34] F. Staub, *SARAH 3.2: Dirac gauginos, UFO output and more*, *Comput. Phys. Commun.* **184** (2013) 1792 [arXiv:1207.0906] [INSPIRE].

[35] F. Staub, *SARAH 4: a tool for (not only SUSY) model builders*, *Comput. Phys. Commun.* **185** (2014) 1773 [arXiv:1309.7223] [INSPIRE].

[36] F. Staub, T. Ohl, W. Porod and C. Speckner, *A tool box for implementing supersymmetric models*, *Comput. Phys. Commun.* **183** (2012) 2165 [arXiv:1109.5147] [INSPIRE].

[37] W. Porod, *SPheno, a program for calculating supersymmetric spectra, SUSY particle decays and SUSY particle production at e^+e^- colliders*, *Comput. Phys. Commun.* **153** (2003) 275 [hep-ph/0301101] [INSPIRE].

[38] W. Porod and F. Staub, *SPheno 3.1: extensions including flavour, CP-phases and models beyond the MSSM*, *Comput. Phys. Commun.* **183** (2012) 2458 [arXiv:1104.1573] [INSPIRE].

[39] W. Porod, F. Staub and A. Vicente, *A flavor Kit for BSM models*, *Eur. Phys. J.* **C 74** (2014) 2992 [arXiv:1405.1434] [INSPIRE].

[40] D.V. Forero, M. Tortola and J.W.F. Valle, *Neutrino oscillations refitted*, *Phys. Rev.* **D 90** (2014) 093006 [arXiv:1405.7540] [INSPIRE].

[41] A. Vicente, *Lepton flavor violation beyond the MSSM*, *Adv. High Energy Phys.* **2015** (2015) 686572 [arXiv:1503.08622] [INSPIRE].

[42] MEG collaboration, A.M. Baldini et al., *Search for the lepton flavour violating decay $\mu^+ \to e^+\gamma$ with the full dataset of the MEG experiment*, *Eur. Phys. J.* **C 76** (2016) 434 [arXiv:1605.05081] [INSPIRE].

[43] SINDRUM collaboration, U. Bellgardt et al., *Search for the decay $\mu^+ \to e^+e^+e^-$*, *Nucl. Phys.* **B 299** (1988) 1 [INSPIRE].

[44] SINDRUM II collaboration, C. Dohmen et al., *Test of lepton flavor conservation in $\mu \to e$ conversion on titanium*, *Phys. Lett.* **B 317** (1993) 631 [INSPIRE].

[45] A.M. Baldini et al., *MEG upgrade proposal*, arXiv:1301.7225 [INSPIRE].

[46] A. Blondel et al., *Research proposal for an experiment to search for the decay $\mu \to eee$*, arXiv:1301.6113 [INSPIRE].

[47] PRIME working group collaboration, S. Machida et al., *A letter of intent to the J-PARC 50GeV proton synchrotron experiment*, http://www-ps.kek.jp/jhf-np/LOIlist/pdf/L25.pdf (2003).

[48] MU2E collaboration, G. Pezzullo, *The Mu2e experiment at Fermilab: a search for lepton flavor violation*, *Nucl. Part. Phys. Proc.* **285-286** (2017) 3 [arXiv:1705.06461] [INSPIRE].

[49] J. Alwall et al., *The automated computation of tree-level and next-to-leading order differential cross sections and their matching to parton shower simulations*, *JHEP* **07** (2014) 079 [arXiv:1405.0301] [INSPIRE].

JHEP01(2018)009